

## The Mysterious Pseudogap in High Temperature Superconductors: An Infrared View.

T. Timusk

Department of Physics and Astronomy, McMaster University, Hamilton ON Canada, L8S 4M1

We review the contribution of infrared spectroscopy to the study of the pseudogap in high temperature superconductors. The pseudogap appears as a depression of the frequency dependent conductivity in the c-axis direction and seems to be related to a real gap in the density of states. It can also be seen in the Knight shift, photoemission and tunneling experiments. In underdoped samples it appears near room temperature and does not close with temperature. Another related phenomenon that has been studied by infrared is the depression in the ab-plane scattering rate. Two separate effects can be discerned. At high temperatures there is broad depression of scattering below  $1000\text{ cm}^{-1}$  which may be related to the gap in the density of states. At a lower temperature a sharper structure is seen, which appears to be associated with scattering from a mode at  $300\text{ cm}^{-1}$ , and which governs the carrier life time at low temperatures. This mode shows up in a number of other experiments, as a kink in ARPES dispersion, and a resonance at  $41\text{ meV}$  in magnetic neutron scattering. Since the infrared technique can be used on a wide range of samples it has provided evidence that the scattering mode is present in all high temperature cuprates and that its frequency in optimally doped materials scales with the superconducting transition temperature. The lanthanum and neodymium based cuprates do not follow this scaling and appear to have depressed transition temperatures.

PACS numbers: 74.25.Kc, 74.25.Gz, 74.72.-h

## INTRODUCTION

Infrared spectroscopy has been used in superconductivity since the 1950's when Tinkham et al. first measured the size of the energy gap in lead with a prism spectrometer using a mercury arc for a radiation source [1]. This was well before the appearance of the BCS theory of superconductivity. The second seminal experiment was the observation of phonon structure, again in the reflectance spectra of strong coupling superconductor lead [2, 3, 4, 5], in 1972. By this time the optical properties of the BCS superconductors were well understood [6, 7] and the phonon structure had been predicted [8]. The superconducting gap can only be observed in the infrared in the dirty limit,  $1 = 2$  where  $1 =$  is the elastic scattering rate of the carriers and  $2$  is the superconducting gap. In this limit direct pairbreaking across the energy gap gives rise to a threshold in absorption at  $h = 2$  where  $h$  is the photon energy [6] and a corresponding "knee" in reflectance spectra. In a clean limit BCS superconductor there is also a knee in the reflectance spectrum but at a higher frequency,  $h = 2 + h$  where  $h$  is the frequency of the boson that is needed to conserve momentum in the absence of impurities. This knee represents the onset of inelastic processes and the spectrum of bosons responsible can be obtained by taking the second derivative of the reflectance spectrum [7, 9]. In a typical BCS superconductor there are two peaks in this spectrum, one for transverse and one for longitudinal phonons. The first derivative of the difference in reflectance between the superconducting and normal states can also be used to extract the boson spectral function [3].

The ab plane reflectance spectra of the high temperature superconductors also exhibits a knee at  $h = 8k_B T_c$ .

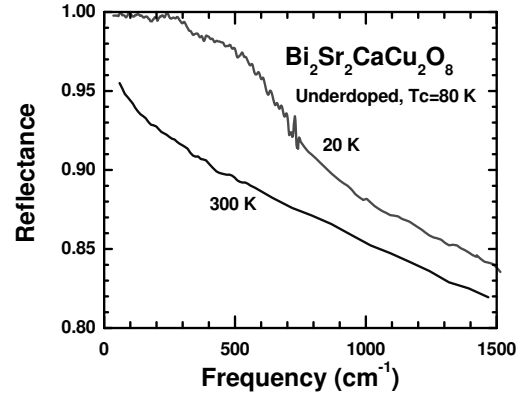


FIG. 1: Infrared reflectance of a typical high temperature superconductor with light polarized along the highly conducting ab-planes. At room temperature the spectrum is Druide-like at low frequency but at high frequency the spectrum does not attenuate, evidence of the presence of high frequency absorption processes. At low temperature and low frequency the reflectance approaches unity over a frequency scale of the order of  $500\text{ cm}^{-1}$  suggestive of a gap-like depression of scattering. In underdoped samples this gap appears well above the superconducting transition temperature.

at low temperature as shown in Fig. 1. However, this is not a signature of the superconducting gap. First, the scattering rate at low temperature is only  $k_B T_c$ , which puts them materials in the clean limit where the gap cannot be seen, [10, 11] and second, at least in underdoped samples, the knee already appears in the normal state [12]. We now know that the knee is a manifestation, not of

the superconducting gap, but the result of a complicated combination of the superconducting gap, the pseudogap and the effect of the boson that seems to dominate transport scattering well above the superconducting transition temperature [13, 14, 15, 16].

The c-axis spectra are also dominated by a reflectance knee but it appears strictly in the superconducting state. Unlike the ab plane knee it is not a result of an onset of enhanced scattering but corresponds to a plasma edge, very much like the plasma edge of silver in the ultraviolet [17]. This has been identified as the Josephson plasma frequency [18].

Kramers-Kronig analysis of the reflectance shows that the optical conductivity is highly anisotropic, it is in the clean limit for transport along the ab-plane and in the dirty limit for c-axis, interplane transport. This leads us to an apparent contradiction: microwave ab-plane measurements [19] show that at least YBCO crystals can be extremely pure with mean free paths extending to microns rivaling the purest of conventional metals. In the same crystals, the c-axis transport is highly incoherent with mean free paths of less than a unit cell. The poor interplane conductivity can not be caused by defects but intrinsic incoherence. Incoherent transport occurs when the probability of in-plane scattering is larger than the probability of interplane charge transfer { the electron has no time to set up a coherent interplane wave function.

A complete review of the optical properties of high temperature superconductors can be found in several recent papers [20, 21]. The more limited purpose of the present paper is to focus on the properties of the pseudogap as seen by infrared spectroscopy and to update recent reviews. However, the earliest evidence of a normal state gap in high temperature superconductors did not come from the optical conductivity but from nuclear magnetic resonance where Warren et al. [22] and Aboulet et al. [23] found evidence of a depressed density of states in the spin excitation spectrum. This gap became known as the spin gap. The first spectroscopic evidence for a pseudogap in high temperature superconductors came from infrared spectroscopy [24]. A pseudogap has been seen with many other experimental probes. These include the Knight shift [25], dc resistivity [26], specific heat [27], angle resolved photoemission (ARPES) [28, 29, 30], tunnelling spectroscopy [31, 32, 33], Raman [34, 35, 36] and neutron scattering [37, 38].

#### THE PSEUDOGAP IN THE C-AXIS CONDUCTIVITY

Homes et al. [24], in a study of the far infrared reflectivity of c-axis oriented  $\text{YBa}_2\text{Cu}_3\text{O}_{x}$  (YBCO), found, superimposed on an otherwise flat background, a gap-like depression of conductivity, which persisted up to

room temperature. Fig 2, top panel, shows the raw data for the c-axis optical conductivity obtained from a Kramers-Kronig transformation of the reflectance of an  $x = 6.60$  sample. The spectrum is dominated by very strong transverse optic phonons. The frequencies and eigenvectors of these phonons are well known from neutron scattering [39]. The lower panel shows the conductivity with the phonons subtracted. We note that at room temperature the spectrum is flat within 5%. This high-temperature background conductivity remains frequency and temperature independent at all doping levels up to optimal doping at  $x = 6.95$  [40].

It is a challenge to theory to account for this simple conductivity behavior, which is entirely unexpected. A simple anisotropic metallic system would show a Drude peak centered at zero frequency. If the observed spectrum is the low frequency end of a broad Drude spectrum with an extremely short relaxation time, a simple calculation would yield a mean free path of less than a lattice spacing, which is in clear contradiction of the long mean free paths seen in the ab-plane conductivity in samples from the same source [19]. On the other hand, there is no sign of a narrow Drude peak that one might expect if the system is an anisotropic metal with a very large mass in the c-direction. At low frequency the observed conductivity is at to less than  $50 \text{ cm}^{-1}$  and the lowest frequency conductivity is in excellent agreement with the dc conductivity, which rules out any sharp Drude peak below the range of far infrared spectroscopy [40, 41]. However, it should be noted that in overdoped samples a rather broad Drude peak appears, which is superimposed on the broad background [42, 43].

There is a large literature that addresses the theoretical problem of this incoherent c-axis response. [44, 45, 46, 47, 48, 49]. Perhaps the most successful are the models that are founded on the original suggestion of Anderson that in analogy with one-dimensional systems, the c axis transport is between two Luttinger liquids. An expression for the conductivity in the one dimensional case is given by Clarke et al. [47]

$$(\sigma) / \sigma^4 \quad (1)$$

where for the 1D Hubbard model  $0 < 4 < 1=4$ . This expression yields a very flat conductivity if a value of  $< 0.2$  is used.

As the temperature is lowered a gap develops in the c-axis conductivity. To see this clearly, the phonon lines have been fitted to Lorentzian profiles and subtracted from the conductivity as shown in the lower panel of Fig. 2. In addition to the phonon lines, the broad peak at  $400 \text{ cm}^{-1}$  that appears at low temperature has also been subtracted. A clear gap-like depression of conductivity is revealed below  $400 \text{ cm}^{-1}$ . Several characteristic features of this c-axis normal state gap should be noted. First, its frequency width does not change with temperature. In other words, the gap does not close as the temperature

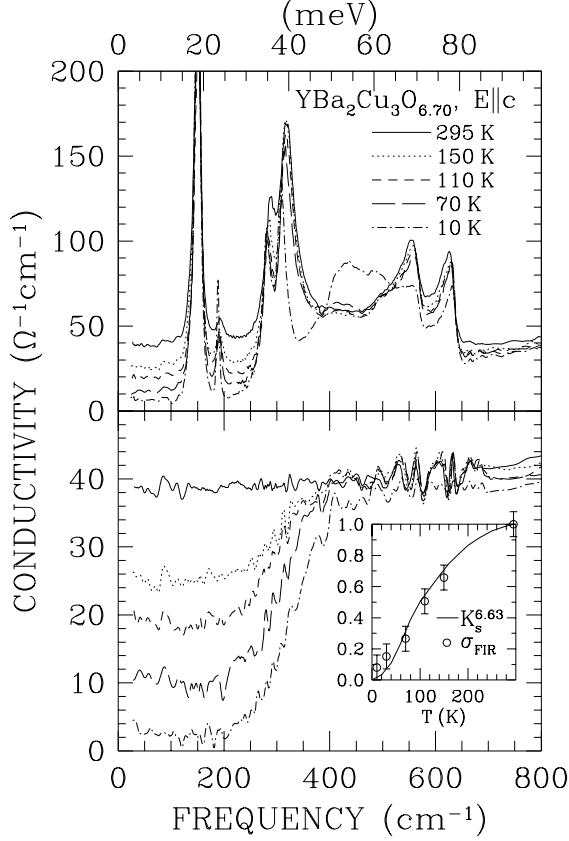


FIG. 2: Optical conductivity measured along the c-axis in  $\text{YBa}_2\text{Cu}_3\text{O}_{6.70}$ . The top panel shows the measured conductivity showing prominent phonon peaks. In the bottom panel these peaks have been subtracted. At high temperature the conductivity is flat and frequency independent. As the temperature is lowered a clear pseudogap is seen below  $400 \text{ cm}^{-1}$ , which appears well above the superconducting transition temperature of 63 K. The amplitude of the gap (open circles) is compared with the NMR Knight shift in the inset.

increases. Instead, as the temperature is raised the depth of the gap decreases up to the point where, at 300 K, the gap has merged with the background conductivity while the frequency scale remains fixed at approximately  $400 \text{ cm}^{-1}$ . Secondly, it is a normal state gap and changes on entry into the superconducting state at  $T_c$  are relatively small. The third striking property is the flatness of the bottom of the gap, which remains flat to high temperatures.

Optimally and overdoped YBCO also show a gap-like depression in low frequency conductivity but the gap appears at  $T_c$  and has been associated with the superconducting gap [24, 43, 50]. This gap does not have the flat bottomed shape of the underdoped materials. Instead, the conductivity rises gradually from a low value at low frequency in a linear fashion to reach the normal state

value in the  $600 \text{ cm}^{-1}$  region.

In this connection it must be pointed out that the non-superconducting ladder compound  $\text{Sr}_{14-x}\text{Ca}_x\text{Cu}_{24}\text{O}_{41}$  [51] where  $x = 11$ , shows a flat bottomed gap normal to the leg direction while the  $x = 8$  sample has a gap similar to the optimally doped YBCO. Note that the  $x = 11$  material has the higher doping and a higher conductivity and is considered to be akin to the optimally doped YBCO. Thus in the ladder compounds the situation is reversed (as the hole doping increases the low temperature gap becomes flatter). This suggests that the shape of the gap at low temperature can not be used as a signature of superconductivity in strongly correlated superconductors.

It has been suggested that the blocking layers play a role in the c-axis transport [48, 49]. In a series of experiments Bernhard et al. [43, 52] on calcium and Pr doped YBCO show that this is not the case. Calcium and praseodymium have the effect of changing the hole doping in the planes without affecting the oxygen content of the chains. Calcium also allows a much larger overdoping of the copper-oxygen planes while keeping the structure of the chains fixed as shown by the ratio of the concentration of four-fold and two-fold coordinated copper chain copper sites. This can be seen by the intensities of the phonons at the corresponding bridging oxygen frequencies [41, 53]. Praseodymium has the opposite effect of reducing the in-plane doping. Bernhard et al. find that the c-axis spectra are independent of the amount of oxygen filling of the chains and depend only on the doping of the planes ruling out models of c-axis transport that involve details of the blocking layers. In the calcium doped materials the authors do find that the overall conductivity in the c-axis direction is higher, which they attribute to the effect of the chains.

On the other hand, substitution of Zn, a strong pair-breaking impurity, which is known to reside on the copper oxygen planes has a strong effect on the c-axis pseudogap spectra [14, 52]. Reducing  $T_c$  with Zn substitution is very different from what happens when  $T_c$  is reduced by underdoping. Basov et al. find that in naturally underdoped two-chain  $\text{YBa}_2\text{Cu}_4\text{O}_8$  (YBCO-124) zinc substitution at the 1.7% level has the effect of eliminating the c-axis pseudogap. This effect of zinc is confirmed by Bernhard et al. who find, in optimally doped  $\text{YBa}_2\text{Cu}_3\text{O}_7$  that at zinc concentration of 6% with  $T_c$  of 64 K, the c-axis spectra show no pseudogap and resemble overdoped samples with a broad Druide component superimposed on the flat c-axis conductivity. In both systems, zinc doping also eliminates the broad peak at  $400 \text{ cm}^{-1}$ . We will return to the role of zinc substitution when we discuss the effect of zinc on ab-plane spectra.

The peak in the conductivity spectrum at  $400 \text{ cm}^{-1}$  was originally interpreted in terms of phonons [24] based on the observation that showed that the overall spectral weight was conserved in the phonon region be-

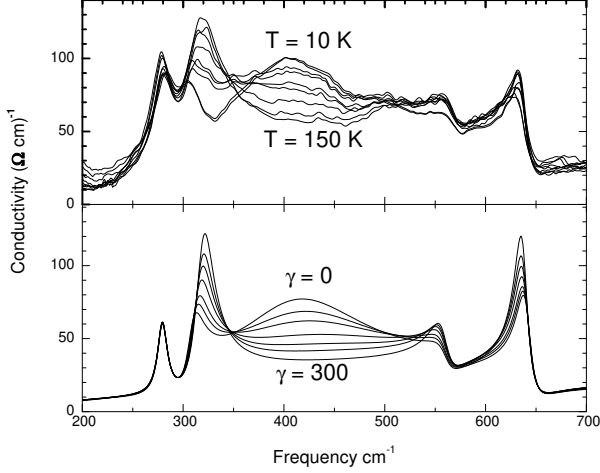


FIG. 3: Interplane conductivity in the oxygen phonon region of underdoped  $\text{YBa}_2\text{Cu}_3\text{O}_7$ , top panel. As the temperature is lowered below 150 K dramatic changes occur in the intensities of the  $\text{CuO}_2$  plane phonon frequencies. At the same time a broad peak centered at  $400 \text{ cm}^{-1}$  grow in spectral weight. The lower panel shows a calculated spectrum based on the interlayer plasmon model of ref. [57] where the damping rate of the interlayer plasmon is allowed to vary.

tween  $250 \text{ cm}^{-1}$  and  $700 \text{ cm}^{-1}$  [41]. In other words, the spectral weight of the peak at low temperature grows at the expense of the spectral weight of some of the phonons. However, more recently a much more satisfactory model has been proposed in terms of an interlayer plasmon [54, 55, 56, 57]. This model takes into account the charge imbalance that is set up in a bilayer system where the conductivity between the bilayers is much larger than between the charge reservoir layers. The model not only explains the mode at  $400 \text{ cm}^{-1}$  but also accounts in detail for the dramatic changes in intensity of certain oxygen phonons [55].

Fig. 3 shows the temperature dependence of the  $400 \text{ cm}^{-1}$  mode in underdoped YBCO, top panel, and a calculation based on the model of Munzar et al. in the bottom panel [57]. It can be seen from the experimental data that the mode makes its appearance below 150 K and thus is not associated with the c-axis pseudogap, which at this doping level, starts to form at room temperature. The calculation in the lower panel is based on the assumption that the temperature dependence of the interlayer plasmon intensity is caused by ab-plane lifetime effects [57].

The frequency-width of the c-axis pseudogap is difficult to establish and there is disagreement about its exact value and its temperature and doping dependence. Homes et al. suggested a pseudogap in the conductivity of  $400 \text{ cm}^{-1}$ , independent of temperature and doping in the doping range of 6.50 to 6.80, with a larger gap in

the optimally doped materials. Bernhard, on the other hand, argued for a larger gap based on c-axis measurements in underdoped Ca doped samples [58]. These discrepancies on gap size arise from the difficulty in performing an accurate subtraction of the phonon background in the  $300$  to  $600 \text{ cm}^{-1}$  region and to the question of whether there is a depression of conductivity beyond the frequency of the highest frequency phonons. Perhaps an analysis that uses details to the interlayer model of Munzar et al. [55] can help to give a more reliable spectroscopy in this frequency region.

More accurate data on the width of the pseudogap can be obtained from ARPES and tunnelling measurements on underdoped  $\text{Bi}_2\text{Sr}_2\text{CaCu}_2\text{O}_8$  (Bi-2212). Both techniques show a clear normal state gap, which persists nearly to room temperature [28, 29, 32, 33]. A larger value of the width of the pseudogap is found [29, 30] with  $2480$  to  $800 \text{ cm}^{-1}$ . In agreement with the infrared data, this gap does not close with temperature but fills in, very much like the gap in the c-axis optical conductivity. An important contribution of the ARPES technique is the finding that the pseudogap develops in the  $(\pi, 0)$  direction in the Brillouin zone and has the same d-wave symmetry as the superconducting gap. The ARPES observation that the normal state gap involves charge carriers away from the nodes is in accord with band structure calculations that show that the matrix element for interplane charge transfer is very small for momenta parallel to  $(\pi, \pi)$  [59, 60, 61]. Thus the c-axis transport involves carriers in the antinodal  $(\pi, 0)$  region.

#### THE PSEUDOGAP AND THE AB PLANE SCATTERING RATE

In many ways measurements of reflectance with infrared polarized in the ab-plane are an ideal way to study low-lying excitations of high temperature superconductors. One reason is a practical one: flux grown single crystals of high temperature superconductors form as thin plates with a large ab-plane area. As a result large ab-plane crystals have been grown for nearly all high temperature superconductors. Also, unlike ARPES and tunnelling techniques, optical techniques are not very surface sensitive.

The onset of absorption at  $500 \text{ cm}^{-1}$  for light polarized in the ab-plane, as seen in Fig. 1, has been attributed to the superconducting gap or the pseudogap. Like the pseudogap as it is seen in the c-axis conductivity, this onset occurs in the normal state and the onset temperature decreases with increased doping. However, it occurs at a much lower temperature than the c-axis pseudogap in the same samples. Also, since the ab-plane transport is coherent the gap cannot be a simple density-of-states effect.

The relationship between a gap in the density of states

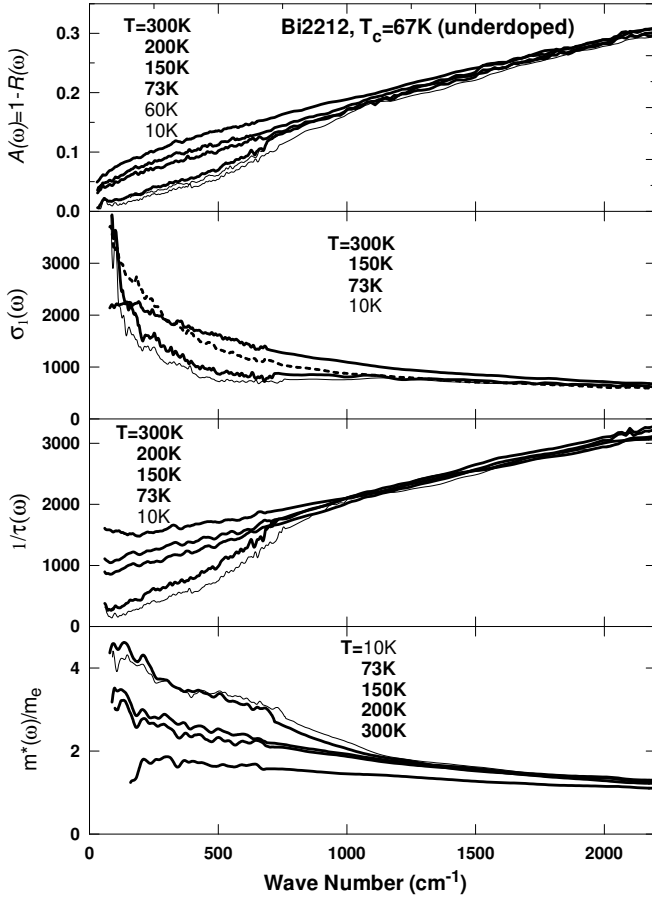


FIG. 4: ab-plane transport properties of underdoped Bi2212. The top panel shows the absorbance, defined as  $1 - R$  where  $R$  is the reflectance. In this strongly underdoped sample an absorption threshold can be discerned at  $600 \text{ cm}^{-1}$ . In the next panel the corresponding optical conductivity is shown. It is approximately Drude-like without a clear gap. The frequency dependent scattering rate, shown in the next panel has a depression below  $600 \text{ cm}^{-1}$ . This depression appears at temperatures below  $150 \text{ K}$ , well above the superconducting transition temperature. The bottom panel shows the mass enhancement.

and an onset of infrared absorption is indirect. The most straightforward way to show this relationship is to first perform Kramers-Kronig analysis on the reflectance to obtain the real and imaginary parts of the conductivity. An example of this kind of analysis is shown in Fig. 4. The absorbance  $A$  of an underdoped sample of Bi2212 with a  $T_c$  of  $67 \text{ K}$  and the optical conductivity are shown from the work of Puchkov et al.[62] While the reflectance shows a clear onset of absorption in the  $600 \text{ cm}^{-1}$  region,

there is no gap in the conductivity. The conductivity looks Drude-like with only a hint of a peak with an onset in the spectral region of the absorption threshold in reflectance. To clearly reveal the presence of any gap it is necessary to look at the frequency dependent scattering rate using the extended Drude model of Allen and Mikkelson.[14, 63]

Based on earlier theoretical work [64, 65] Allen and Mikkelson showed that the Drude formula

$$\epsilon(\omega) = \frac{1}{4} \frac{\omega_p^2}{1 - i\omega\tau} \quad (2)$$

can be extended to include a frequency dependent scattering rate:

$$\epsilon(\omega; T) = \frac{1}{4} \frac{\omega_p^2}{1 - i\omega\tau(\omega; T) [1 + \gamma(\omega; T)]} \quad (3)$$

where  $\tau(\omega; T)$  is the frequency dependent scattering rate and  $\gamma(\omega; T)$  the mass enhancement of the electronic excitations due to the interactions.

One can solve for  $\tau(\omega)$  and  $1 + \gamma(\omega)$  in terms of the optical conductivity found from the experimental reflectivity to find:

$$\tau(\omega) = \frac{\omega_p^2}{4} \text{Re} \left( \frac{1}{\epsilon(\omega)} \right); \quad (4)$$

The dc resistivity is zero frequency limit  $\rho_{dc}(T) = 1/\sigma_{dc}(T) = m_e / (e^2 n)$  since  $\epsilon(\omega)$  is real in the zero frequency limit.

The mass enhancement factor  $\gamma(\omega)$  is the imaginary part of  $1 + \gamma(\omega)$ :

$$1 + \gamma(\omega) = \frac{\omega_p^2}{4} \frac{1}{\omega} \text{Im} \left( \frac{1}{\epsilon(\omega)} \right); \quad (5)$$

The total plasma frequency  $\omega_p^2$  can be found from the sum rule  $\int_0^\infty \epsilon_1(\omega) d\omega = \omega_p^2/8$ . The choice of this arbitrary cut-off introduces an uncertainty to the overall scale factor of the scattering rate and effective mass.

The frequency dependent scattering rate formalism has been used to describe electron-phonon scattering [7, 66]. Shulga et al.[66] give the following expression for  $\tau(\omega; T)$ :

$$\frac{1}{\tau(\omega; T)} = \frac{Z}{\omega} \int_0^\infty d\omega' \omega'^2 F(\omega') \coth\left(\frac{\omega'}{2T}\right) + \left(1 + \frac{\omega}{2T}\right) \coth\left(\frac{\omega}{2T}\right) + \frac{1}{\tau_{imp}}; \quad (6)$$

Here  $F(\omega')$  is a weighted phonon density of states and  $T$  is the temperature measured in frequency units. The last term represents impurity scattering.

The quantity  $\frac{2}{\tau}(\omega)F(\omega)$  is closely related to  $\frac{2}{\tau}(\omega)F(\omega)$  obtained from the inversion of tunnelling spectra in BCS superconductors [7] and it can be found by inverting the optical conductivity spectra at  $T = 0$  [3, 7, 9] to yield:

$$\frac{2}{\tau}(\omega)F(\omega) = \frac{1}{2} \frac{\partial}{\partial \omega} \left( \frac{1}{\tau} \frac{\partial}{\partial \omega} \frac{1}{\tau} \right) : \quad (7)$$

The difficulty with the application of this method to practical spectroscopy arises from the presence of the second derivatives in the expression, which places severe demands on the signal-to-noise ratio of the experimental spectra. Despite this, the method has been applied with considerable success to BCS superconductors to extract  $\frac{2}{\tau}(\omega)F(\omega)$ , to  $K_3C_{60}$  [9] and more recently to high  $T_c$  superconductors [15, 67, 68].

There is an alternative approach to the analysis of infrared data, the two-component model [69, 70]. Here one treats a Drude oscillator to the low frequency component of the conductivity and treats the remaining conductivity as a separate parallel channel of conductivity, the mid-infrared band. This approach is applicable in particular to the La-214 system where such a separate band is more clearly resolved but it has also been used for the cases where there is no obvious separation between the low and high frequency portions of the spectrum [71].

Fig. 4, third and fourth panels from the top, show the scattering rate and the effective mass for the underdoped Bi-2212 system. We see that the scattering rate at room temperature has a linear variation with frequency starting from a rather large constant value  $1280 \text{ cm}^{-1}$ . The scattering rate above  $1000 \text{ cm}^{-1}$  remains temperature independent at its 300 K value but as the temperature is lowered there is a lowering of low frequency scattering between  $T$  and  $T_s$ . At 150 K the scattering rate begins to drop precipitously at low frequency forming a gap-like depression that extends to about  $700 \text{ cm}^{-1}$ . To distinguish its onset temperature from the higher onset temperature of the c-axis pseudogap  $T^*$ , we will call the lower ab-plane onset  $T_s$  [57]. Like the c-axis pseudogap it occurs in the normal state in underdoped samples and at or near  $T_c$  in optimally doped ones [72]. In underdoped systems the change in the scattering rate on entering the superconducting state is small. The lowest panel shows the mass enhancement of the carriers resulting from the frequency dependent scattering.

These general features are seen in all the cuprate systems. A gap in the scattering rate was first identified in YBCO and Bi-2212 systems, materials with two copper-oxygen layers, but it is also seen in the one-layer  $Tl_2Ba_2CuO_{6+}$  (Tl-2201) system [62]. The depression of low frequency scattering has also been reported in  $La_{2-x}Sr_xCu_3O_4$  (La-214) [73, 74, 75] and the three layer  $Hg_2Ba_2CaCu_3O_{8+}$  (Hg-2213) system [76] as well as in the electron doped  $Nd_{2-x}Ce_xCu_3O_{4+}$  (NdCe) [67, 75].

The three layer mercury compound (Hg-1223) is unique in that it has a maximum  $T_c$  of as high as 135 K, which is substantially higher than the intensively studied "canonical" superconductors YBCO and Bi-2212 both with maximum  $T_c$ 's at optimal doping of 93 K. Single crystals of the mercury material are difficult to grow and, and as a result, very few experiments have been done on this system. Infrared spectroscopy on the ab-plane that has been performed by McGuire et al. [76] shows that the material behaves very much like other cuprates with one notable exception: the energy scale for the gap in ab-plane scattering is 40 % higher than in materials with a  $T_c$  of 93 K, in the exact ratio of their transition temperatures. Energy scales measured with other probes such as the  $B_{1g}$  Raman intensity [77] and the copper hyperfine coupling constant measured by NMR [78] are also much higher.

The La-241 material also differs from YBCO and Bi-2212 in that its  $T_c$  at optimal doping is substantially lower than YBCO and Bi-2212. The presence of a pseudogap in this material is somewhat controversial. Magnetic resonance suggests that the pseudogap is unusually weak [79] and the copper spin relaxation time shows no sign of a pseudogap [80]. On the other hand, transport measurements find a suppression of resistivity at a temperature  $T^*$ , which is unusually high [81]. Infrared conductivity in the c-axis direction shows the presence of a pseudogap in the conductivity that starts near room temperature in slightly underdoped samples, but the overall suppression of conductivity is less complete than in the YBCO material [73, 82, 83].

In the ab-plane infrared properties La-241 also shows differences when compared to other cuprates. From its lower superconducting transition temperature one might expect a overall lower frequency scales. This is not the case. The characteristic knee in resistance that signals the onset of scattering is seen in the La-214 material at approximately the same frequency range as in materials with a  $T_c$  of 93 K [73, 74]. The exact frequency of this feature is difficult to discern due to the presence of c-axis longitudinal phonon lines induced by structural defects [84, 85]. Recent experiments with better crystals [75] suggest the gap in the scattering rate in La-214 is around  $1000 \text{ cm}^{-1}$ , similar to that in superconductors with higher transition temperatures but it is difficult to separate this energy scale from the lower scale caused by the resonance as shown in Fig. 4 for Bi-2212.

Because the ab-plane conductivity is metallic and approximately Drude-like, the gap-like depression seen in the scattering rate cannot simply be interpreted as a gap in the density of states. As the frequency dependent scattering rate formalism suggests, we must look to models that describe the scattering rate. The most successful of these have been the marginal Fermi liquid model (MFL) of Varma et al. [86] at high temperatures and the scattering of carriers by a bosonic excitation [13, 15, 16, 96] at

low temperatures. It must be pointed out however that the models that invoke a bosonic excitation to account for the onset of scattering at  $T_s$  are based on Fermi liquid ideas with well defined quasiparticles. As an inspection of the scattering rates shown in Fig. 4 shows that for this material at least the scattering rate is higher than the frequency at all temperatures.

As Fig. 4 shows, the scattering rate in underdoped Bi-2212 at room temperature is quite remarkable with a frequency variation that is accurately linear up to at least  $2000 \text{ cm}^{-1}$ . It is worth pointing out that a Drude model predicts a constant scattering rate as a function of frequency and any model involving bosonic excitation would have characteristic features at the frequency of these excitations. This simple featureless linear behavior can be seen in all cuprate materials and at all doping levels and is closely related to another remarkable property of the cuprates, their linear variation of resistivity with temperature [87]. The semi-empirical MFL model of Varnam et al. [86] attempts to account for these properties by assuming that the electron self-energy  $\Sigma(k; \omega)$  rate is given by:

$$\text{Im} \Sigma(k; \omega) = g^2 N(0) \ln \frac{\omega}{\omega_c} \quad (8)$$

where  $g$  is a coupling constant,  $N(0)$  the density of states at the Fermi surface,  $\omega_c$  a high frequency cut-off and  $\omega = \max(|\omega|, T)$ . This expression fits the experimental data well in the high temperature region [86, 88] but fails in the underdoped region at low temperatures since it does not include the gap-like depression in scattering below the  $T_s$  temperature.

It is clear from Fig. 4 that, as the temperature is lowered, a gap develops in the scattering rate below  $300 \text{ K}$  [89]. The gap has the effect of reducing the scattering below the marginal Fermi liquid line. In optimally doped samples of YBCO this temperature is very close to the superconducting transition temperature [14], while in Bi-2212 it is clearly above  $T_c$  [62, 68]. However, while a gap in scattering may be caused by a gap in the density of states, as for example in the case of simple electron-electron scattering, it is now clear that this model does not account all the experimental data in underdoped cuprates. As the data in Fig. 4 show, the gap in the scattering rate in underdoped Bi-2212 first sets in the around room temperature with a frequency scale of the order of  $1000 \text{ cm}^{-1}$  followed by a more rapid decrease in neighborhood of  $150 \text{ K}$ . The lower temperature gap can be understood, in analogy with the electron-phonon interaction in conventional superconductors [7], where the scattering by a bosonic mode is invoked to account for the onset of scattering in the  $500 \text{ cm}^{-1}$  region.

An early attempt along these lines was the work of Thomas et al. [13] and Puchkov et al. [72] who found that a broad bosonic peak in the  $300 \text{ cm}^{-1}$  region could account for the scattering rate variation with frequency although

not with temperature. More recently, Marsiglio showed that one could extract the spectral density of this mode  $W(\omega)$  from the experimental data by taking the second derivative of the scattering rate [9]:

$$W(\omega) = \frac{1}{2} \frac{d^2}{d\omega^2} \frac{\text{Im} \Sigma(k; \omega)}{\omega} \quad (9)$$

This method has been successfully applied to the scattering rate spectra of  $\text{CeCu}_2\text{Si}_2$  [9], to YBCO [15, 90]. This analysis did not account too well for a region of negative  $W(\omega)$  seen above the broad peak in the superconducting state.

Abanov et al. [16] showed that the negative peak was not only expected but gave an independent measure of the superconducting gap. Using the method of Abanov, Tu et al. analyzed very high quality reflectance data on optimally doped Bi-2212 [68] and were able to deduce a value of the superconducting gap  $\Delta = 30 \pm 4 \text{ meV}$  and a resonance  $\omega_{sr} = 40 \pm 4 \text{ meV}$  ( $322 \text{ cm}^{-1}$ ) in excellent agreement with tunnelling data at  $\Delta = 27 \text{ meV}$  and the mode seen in magnetic neutron scattering  $\omega_{sr} = 41 \text{ meV}$  [91]. In the normal state, the peak is seen at a frequency corresponding to the resonance mode and the peak persists at least up to  $100 \text{ K}$  and the negative going feature due to superconductivity can not be seen. These results are in accord with the observation that in optimally doped  $\text{YBa}_2\text{Cu}_3\text{O}_{7-x}$  where the infrared mode is not seen in the normal state and turns on sharply at  $T_c$  [62]. However, we note that while in optimally doped Bi-2212 a clear kink was seen in the scattering rate at  $T_c$  whereas the YBCO spectrum was flat and featureless at  $95 \text{ K}$ , a few degrees above  $T_c$ . This suggests that in optimally doped  $\text{YBa}_2\text{Cu}_3\text{O}_{7-x}$  the mode-scattering onset temperature  $T_s = T_c$ , while in Bi-2212  $T_s > T_c$ .

To further investigate the systematics of the bosonic mode, we plot in Fig. 5 the frequency of the peak in  $W(\omega)$  at low temperature as a function of  $T_c$  for several optimally doped cuprate systems. Most of the data are from a recent paper by Singley et al. [67] with added data on Tl-2212 from the work of Tanner [92]. Two features stand out. First, for most high  $T_c$  systems the points cluster at  $T_c = 93 \text{ K}$  and peak frequency of  $550 \text{ cm}^{-1}$ . However, if the data from the mercury and the two layer thallium materials are included, there is a trend for the system with higher  $T_c$  towards a linear dependence with a regression line that goes through the origin. Within the bosonic model, this means that at optimal doping the sum of the superconducting gap and the resonance frequency is proportional to  $T_c$ .

The second notable feature of Fig. 5 is that the linear variation does not apply to the LaSr and NdCe systems. While the systems do exhibit a peak at reasonably high frequency, their  $T_c$  seems to be suppressed as compared to the systems with higher transition temperatures. We note that this is not an effect of double vs. single layers since one of the systems that falls on the line is the one-layer Tl-2201 system. The  $T_c$  suppression in the LaSr

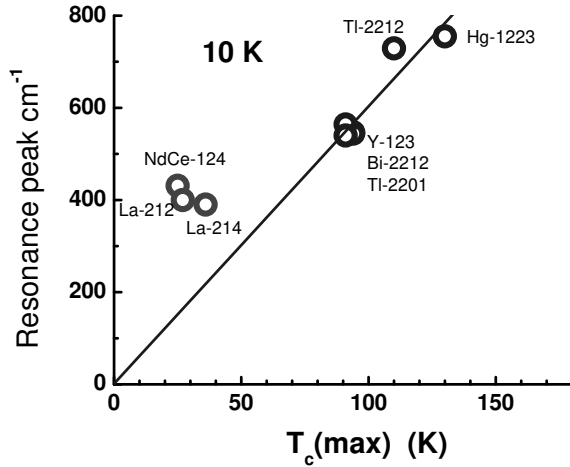


FIG. 5: The frequency of the ab-plane scattering resonance as a function of  $T_c$  for optimally doped high  $T_c$  superconductors. The straight line is a fit to the superconductors with a  $T_c$  above 90 K. Included in this group is the one-plane Ti-2201. The LaSr-214 and NdCe-214 do not follow on this line.

system may be due to the disorder introduced by the La dopant ions. But it is also possible that the model of scattering by a well defined mode is not appropriate for these systems and that the gap-like depression of scattering is due to the combination of a pseudogap and a broad mode. In this context it is worth pointing out that the neutron mode has not been seen in these systems.

The bosonic mode model is expected to give rise to a kink in the dispersion curves of the charge carriers [93, 96] and this kink has indeed been observed in ARPES dispersion curves [94, 95], which further confirms the overall picture of the kink. The frequency of the kink in ARPES dispersion is in fairly good agreement with the frequency of the bosonic mode deduced from optical spectra [96] and its temperature dependence is in general agreement with what is seen in optical spectra.

While the picture of the bosonic mode explains a number of features in infrared and ARPES spectra, it does not provide a complete theory of the interactions of the holes in high temperature superconductors since the model tells us nothing about the nature of the mode. Carbotte et al. [15] proposed that the 41 meV neutron mode is the responsible agent. Lanzara et al. on the other hand, have made the suggestion recently that the mode is due to an in-plane copper-oxygen vibration. [97] We will examine these ideas in turn.

The picture of the neutron mode as the cause of the gap-like depression of the ab-plane scattering rate below a temperature  $T_s$  and the kink in the ARPES dispersion spectra has several attractive features. The frequency of the neutron peak is in good agreement with the observed

position of the infrared features [15, 68] in systems where the neutron peak has been seen. Unfortunately this is not a good test since, as Fig. 5 shows, all these systems have the same frequency scale. The crucial test, the observation of the neutron peak in the three layer mercury compound, is very difficult because of the lack of large enough crystals for magnetic neutron scattering.

Secondly, the temperature where the neutron peak appears is in accord with the onset temperature  $T_s$  of depressed ab-plane scattering [72] although there is an unfortunate lack of data in the crucial temperature region between 200 K and  $T_c$  where the gap in the scattering rate makes its appearance. It is clear that more work is needed to settle this question. ARPES spectra also show that the kink and the accompanying decrease in scattering at low temperature are consistent with the neutron mode picture but the ARPES data are also very sparse along the temperature axis.

The alternate picture of a phononic origin of the mode is more difficult to accept. First of all, the mode frequency does not show the isotope effect expected for phonons [98]. Secondly, since the mode frequency scales with  $T_c$  as shown in Fig. 5, which is the sum of the gap frequency and the mode frequency, it is difficult to understand the 40% increase in this sum in the three layer mercury compound in the phonon picture since copper-oxygen in-plane phonon frequencies do not change substantially from one material to another. Also, quantitatively, phonon models based on a Fermi liquid approach fail completely when it comes to the temperature dependence of the scattering rate [67, 72]. The neutron mode, unlike the phonons, has a strongly temperature dependent spectral function, which essentially vanishes at a temperature not far above  $T_s$  into the general magnetic background.

Further support for a magnetic origin of the mode is offered by Zn doping experiments. Recent experiments [99] show that Zn doping has the effect of reducing the width of the neutron mode while leaving the overall spectral weight unchanged. This is in accord with the general picture of zinc as a strong in-plane scattering center as seen from the strong effect of zinc on both  $T_c$  and resistivity. The ab-plane scattering rate spectra of Basov et al. [14] confirm this picture for the naturally underdoped system of YBCO-124. In the undoped material the scattering rate increases sharply  $350 \text{ cm}^{-1}$  followed by a broader threshold at  $500 \text{ cm}^{-1}$ , which is very similar to what happens in other underdoped materials. With 0.425% zinc doping the sharp onset structure is completely obliterated but an overall depression of low frequency scattering remains and is spread out over a frequency interval of the order of  $1000 \text{ cm}^{-1}$ . This doping level is evidently high enough to suppress the scattering by a well defined mode but retain the influence of the pseudogap in the density of states. Further doping to 1.275% zinc has the interesting effect of completely suppressing superconductivity



and eliminating any gap-like structure in the scattering rate spectra, which makes them look very much like the spectra in the normal state of optimally doped YBCO where the neutron mode is absent.

Similar effects are found by Zheng et al. in NMR experiments on YBCO-124 doped with zinc [100, 101]. While Zn doping has a relatively small effect on the Knight shift, it completely suppresses the pseudogap in the spin relaxation rate already at the 1% doping level.

#### EVIDENCE FOR TWO CHARACTERISTIC ENERGY SCALES.

All experimental techniques used to study the cuprates show evidence of a pseudogap in underdoped materials [21]. Common features include a decreasing onset temperature  $T^*$  with doping, a temperature that appears to merge with the superconducting transition temperature at or near optimal doping. However, early on there was evidence from NMR experiments for two energy scales, a higher one seen in the  $q = 0$  susceptibility as revealed by the Knight shift, and a lower one related to the  $1/T_1 T$  susceptibility of the relaxation rate  $1/T_1 T$  [102]. Generally the Knight shift is considered to be a measure of the density of states whereas the relaxation rate measures the carrier lifetime.

That the gap in the c-axis optical conductivity and the NMR Knight shift may have a common origin can be seen from the temperature scale of the Knight shift and the optical conductivity shown as the inset of Fig. 2 where both extend to almost room temperature in the underdoped YBCO with  $T_c = 60$  K. A similar correspondence has been found for the double chain compound YBCO-124 [103]. The broad suppression of frequency dependent scattering with the  $1000 \text{ cm}^{-1}$  frequency scale seen in Bi-2212 must also be included in this class of phenomena.

However, there is good evidence for another class of phenomena with a lower temperature and frequency scale. In the underdoped YBCO  $T_c = 60$  K material, the onset of several physical quantities relating to the lifetime of the in-plane excitations occur at a much lower temperature, in the 150 K region, and they have their most rapid change at  $T_c$ . This is illustrated in Figs. 6 and 7 from a recent paper of Timusk and Homes [57] where in addition to the NMR Knight shift and the relaxation  $1/T_1 T$ , the c-axis pseudogap amplitude and the amplitude of the c-axis infrared mode at  $400 \text{ cm}^{-1}$  have been plotted.

It can be seen from Fig. 6 that the various plotted quantities fall into two groups: first there are those that have an onset near room temperature and show a rather gradual development of the amplitude as the temperature is lowered with no rapid changes at the superconducting transition temperature. They include the c-axis pseudogap and the NMR Knight shift. Not plotted here is the

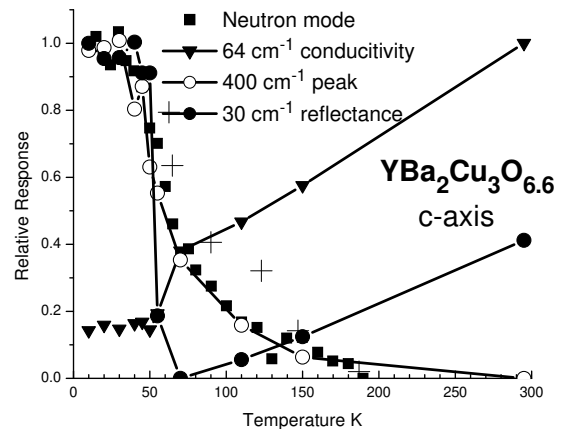


FIG. 6: Three temperature scales can be identified in underdoped  $\text{YBa}_2\text{Cu}_3\text{O}_{7-x}$ . The largest is around 300 K and is associated with the pseudogap, which is approximated as the conductivity at  $64 \text{ cm}^{-1}$  in c-axis transport. The next governs the intensity of the  $400 \text{ cm}^{-1}$  peak and neutron mode. It has a value of approximately 150 K as well as NMR relaxation, not shown here. The lowest one is associated with superconductivity and has a value of 60 K in this underdoped sample. We use the  $30 \text{ cm}^{-1}$  reflectance to approximate the superconducting condensate density. The crosses show an estimate of the  $400 \text{ cm}^{-1}$  peak amplitude based on broadening by in-plane scattering as shown in Fig. 3.

tunnelling density of states, which also shows a pseudogap that also follows the higher energy scale [32, 33].

Then there is a second group of quantities that start at 150 K and change rapidly near the superconducting transition temperature. These include the relaxation  $1/T_1 T$ , the amplitude of the c-axis peak at  $400 \text{ cm}^{-1}$  and the  $41 \text{ meV}$  neutron resonance.

At this stage it is not possible at this point to conclusively fit the ab-plane scattering rate data into this picture. From the existing data it appears that suppression of ab-plane scattering is caused by both the high temperature phenomena in the form of the broad depression of scattering with the  $1000 \text{ cm}^{-1}$  scale and the low temperature gap in scattering associated with the bosonic mode. There is lack of relevant data not only for the infrared scattering rate but also for the kink in ARPES dispersion and dc transport. More work is needed to settle this question. However there are strong hints from the available data that the ARPES kink and the ab-plane scattering rate gap from the bosonic mode both belong to the low temperature group while the ARPES d-wave gap at  $(\pi, \pi)$  [104] and the Knight shift along with with the  $1000 \text{ cm}^{-1}$  depression of conductivity follow the high temperature scale.

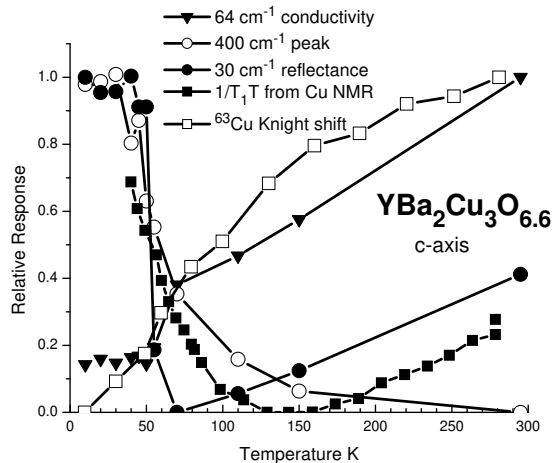


FIG. 7: Infrared pseudogap and magnetism in underdoped YBCO. The amplitude of the Knight shift plotted as open squares and the pseudogap plotted as triangles and approximated here as the  $64 \text{ cm}^{-1}$  conductivity. The Knight shift depression starts at room temperature in this sample with an oxygen content of 6.60. The relaxation time, shown as solid squares, is plotted as  $[1 - (T_1/T)]$ . It starts to deviate from the uniform high temperature form at around 150 K and is better to the  $400 \text{ cm}^{-1}$  peak intensity than the Knight shift.

#### SUMMARY

We have discussed two separate experiments where infrared spectroscopy shows evidence of a gap-like depression in physical quantities in underdoped cuprates, the c-axis conductivity and the ab-plane scattering rate. The depression of the c-axis conductivity seems to be associated with a real gap in the density of states as shown by the Knight shift, ARPES and tunnelling and possibly the  $1000 \text{ cm}^{-1}$  scale ab-plane scattering rate suppression. This pseudogap appears near room temperature in samples where  $T_c$  has been reduced to 60 K, has width that does not change with temperature and seems to merge with the superconducting gap near optimal doping. The gap associated with a depressed scattering rate in the ab-plane transport with the  $600 \text{ cm}^{-1}$  frequency scale shows up at a lower temperature and appears to be associated with scattering from a mode. ARPES dispersion shows this mode to be present in Bi-2212 and there is good evidence that the 41 meV neutron mode is the responsible agent, although the idea that phonons may be involved has also been advanced. To confirm this picture of a gap and a distinct mode, a detailed study of the temperature dependence of the two phenomena in the same system is needed. Underdoped YBCO seems to be a good candidate for this since at least two groups are able to grow thick, high-quality crystals of this material [105].

#### ACKNOWLEDGEMENTS

First and foremost I would like to thank my long term collaborators who have made this work possible. These include Doug Bonn, David Tanner, Maureen Reedyk, John Greedan, Chris Homes, Dimitris Basov and Anton Puchkov. More recently Tatiana Startseva, Jeannette McGuire, Nan Lin Wang, Thomas Room and Jungseok Hwang have made enormous contributions by developing the capability to work with more and more difficult samples. My colleagues Elihu Abrahamson, Phil Anderson, John Berlinsky, Jules Carbotte, Takashi Inai, Steve Kivelson, Catherine Kallin, Patrick Lee, Kathy Levin, Frank Marsiglio, Thomas Mason, Andy Millis, Mike Norman, David Pines, Louis Taillefer and Mike Walker have provided valuable insight into the mysteries of the pseudogap in high temperature superconductors.

The Canadian Institute of Advanced Research; Electronic address: tinusk@mcmaster.ca

- [1] R.E. Glover and M. Tinkham, Phys. Rev. B 107, 844, 1956; ibid, 108, 1175 (1957).
- [2] R.R. Joyce and P.L. Richards, Phys. Rev. Lett. 24, 1007 (1970).
- [3] B. Farnworth and T. Timusk, Phys. Rev. B 10, 2799, (1974).
- [4] B. Farnworth and T. Timusk, Phys. Rev. B 14, 5119 (1976).
- [5] G. Brandli and A.J. Sievers, Phys. Rev. B 5, 3550 (1972).
- [6] D.C. Mattis and J. Bardeen, Phys. Rev. 111, 412 (1958).
- [7] P.B. Allen, Phys. Rev. B 3, 305 (1971).
- [8] S.B. Nam, Phys. Rev. 156, 470, 487 (1967).
- [9] F. Marsiglio, T. Startseva, J.P. Carbotte, Phys. Lett. A 245, 354 (1998).
- [10] T. Timusk, S.L. Herr, K. Kamaras, C.D. Porter, D.B. Tanner, D.A. Bonn, J.D. Garrett, C.V. Stager, J.E. Greedan, and M. Reedyk, Phys. Rev. B 38, 6683 (1988).
- [11] K. Kamaras, S.L. Herr, C.D. Porter, N. Tache, D.B. Tanner, S. Etemad, T. Venkatesan, E. Chase, A. Inam, X.D. Wu, M.S. Hegde, and B. Dutta, Phys. Rev. Lett. 64, 84 (1990).
- [12] M. Reedyk, D.A. Bonn, J.D. Garrett, J.E. Greedan, C.V. Stager, T. Timusk, K. Kamaras, and D.B. Tanner, Phys. Rev. B 38, 11981 (1988).
- [13] G.A. Thomas, J. Orenstein, D.H. Rapkine, M. Capizzi, A.J. Millis, R.N. Bhatt, L.F. Schneemeyer, and J.V. Waszczak, Phys. Rev. Lett. 61, 1313 (1988).
- [14] D.N. Basov, R. Liang, B. Dabrowski, D.A. Bonn, W.N. Hardy, and T. Timusk, Phys. Rev. Lett. 77, 4090 (1996).
- [15] J.P. Carbotte, E. Schachinger, and D.N. Basov, Nature 401, 354 (1999).
- [16] A. Abanov, A.V. Chubukov, and J. Schmalian, Phys. Rev. B 63, 180510 (2001).
- [17] D.A. Bonn, J.E. Greedan, C.V. Stager, T. Timusk, M.G. Dressel, S.L. Herr, K. Kamaras, C.D. Porter, D.B.

- Tanner, J.M., Tarascon, W.R.McKinnon, and L.H. Greene, *Phys. Rev. B* 35, 8843, (1987).
- [18] K. Tamasaku, Y. Nakamura, and S. Uchida, *Phys. Rev. Lett.* 69, 1455 (1992).
- [19] D.A. Bonn, P. Dosanjh, R. Liang, and W.N. Hardy, *Phys. Rev. Lett.* 68, 2390 (1992).
- [20] D.N. Basov, and T. Timusk, *Infrared Properties of High- $T_c$  Superconductors: an Experimental Overview in Handbook on the Physics and Chemistry of Rare Earths*, Vol 31, Edited by K.A.G. Schneider, Jr., L. Eyring and M.B. Maple, Elsevier Science BV, 2001 pp. 437-507, (2001).
- [21] T. Timusk and B. Statt, *Reports of Progress in Physics* 62, 61 (1999).
- [22] W.W. Warren, Jr., R.E. Walstedt, G.F. Brennert, R.J. Cava, R. Tycko, R.F. Bell, and G.D. Abbagh, *Phys. Rev. Lett.* 62 1193, (1989).
- [23] H. Aloul, T. Ohno, and P. Mendels, *Phys. Rev. Lett.* 63, 1700 (1989).
- [24] C.C. Homes, T. Timusk, R. Liang, D.A. Bonn, and W.N. Hardy, *Phys. Rev. Lett.* 71, 1645 (1993).
- [25] R.E. Walstedt, R.F. Bell, R.J. Cava, G.P. Espinosa, L.F. Schneemeyer, and J.V. Waszczak, *Phys. Rev. B* 41, 9574 (1990).
- [26] B. Bucher, P. Steiner, J. Karpinski, E. Kalkis, and P. Wachter, *Phys. Rev. Lett.* 70, 2012 (1993).
- [27] J.W. Loram, K.A. Mirza, J.R. Cooper, and W.Y. Liang, *J. of Superconductivity*, 7, 261 (1994).
- [28] A.G. Loeser, Z.-X. Shen, D.S. Dessau, D.S. Marshall, C.H. Park, P. Fournier, and A. Kapitulnik, *Phys. Rev. Lett.* 76, 4841 (1996).
- [29] H. Ding, T. Tokoya, J.C. Campuzano, T. Takahashi, M. Randeria, M.R. Norman, T. Mochiku, K. Kadowaki, and J. G. Japitzakis, *Nature* 382, 51 (1996).
- [30] D.S. Marshall, D.S. Dessau, A.G. Loeser, C.H. Park, Z.-X. Shen, A.Y. Matsuura, J.N. Eckstein, I. Bozovic, P. Fournier, A. Kapitulnik, W.E. Spicer, and Z.-X. Shen, *Phys. Rev. Lett.* 76, 4841 (1996).
- [31] H.J. Tao, F. Lu, and E.L. Wolf, *Physica C* 282-287 1507 (1997).
- [32] Ch. Renner, B. Revaz, J-Y Genoud, K. Kadowaki, and O. Fischer *Phys. Rev. Lett.* 80, 149, (1998).
- [33] V.M. Krasnov, A. Yurgens, D. Winkler, P. Delsing, and T. Claeson, *Phys. Rev. Lett.* 84, 5860 (2000).
- [34] F. Slakey, M.V. Klein, J.P. Rice, and D.M. Ginsberg, *Phys. Rev. B* 42, 2643 (1990).
- [35] R. Hackl, G. Kug, R. Nemetschek, M. Opel, and B. Stadlober, in *Spectroscopic Studies of Superconductors V*, Ivan Bozovic and Dirk van der Marel, Editors, *Proc. SPIE* 2696, 194 (1996).
- [36] J.G. Naeini, X.K. Chen, J.C. Irwin, M. Okuya, T. Kinura, and K. Kishio *Phys. Rev. B* 59, 9642 (1999).
- [37] J. Rossat-Mignod et al. *Physica C* 185-189, 86 (1991).
- [38] J.M. Tranquada et al. *Phys. Rev. B* 46, 5561 (1992).
- [39] T. Timusk, C.C. Homes, and W. Reichardt, *Int. Workshop on the Anharmonic Properties of High  $T_c$  Cuprates*, Bled, Slovenia, G. Ruani, editor (World Scientific, Singapore, 1995).
- [40] C.C. Homes, T. Timusk, R. Liang, D.A. Bonn, and W.H. Hardy, *Can. J. Phys.* 73, 663, (1995).
- [41] C.C. Homes, T. Timusk, R. Liang, D.A. Bonn, and W.H. Hardy, *Physica C*, 254, 265-280, (1995).
- [42] J. Schutzmann, S. Tajima, S. Miyamoto, and S. Tanaka, *Phys. Rev. Lett.* 73, 174 (1994).
- [43] C. Bernhard, R. Henn, A. W. Ittlin, M. K. Kaser, Th. Wolf, G. Müller-Vogt, C.T. Lin, and M. Cardona, *Phys. Rev. Lett.* 80, 1762, (1998).
- [44] N. Kumar and A.M. Jayannavar, *Phys. Rev. B* 50, 438 (1992).
- [45] S. Chakravarty et al. *Science* 261, 337 (1993).
- [46] A.G. Rojo and K. Levin, *Phys. Rev. B* 48, 16861 (1993).
- [47] D.G. Clarke, S.P. Strong, and P.W. Anderson, *Phys. Rev. Lett.* 74, 4499 (1995).
- [48] A.A. Abrikosov, *Phys. Rev. B* 54, 12003 (1996).
- [49] W.A. Atkinson, *Phys. Rev. B* 59, 3377 (1999).
- [50] B. Koch, M. Dürler, H.P. Gessrich, Th. Wolf, G. Roth, and G. Zschmann, in *Electronic Properties of High- $T_c$  Superconductors and Related Compounds*, ed. H. Kuzmany, M. Mehrig, J. Fink (Springer Series in Solid State Sciences, Vol 99, Springer-Verlag, Berlin - Heidelberg, 1990), p. 290.
- [51] T. Osafo, N. Motoyama, H. Eisaki, S. Uchida, and S. Tajima *Phys. Rev. Lett.* 82, 1313 (1999).
- [52] C. Bernhard, T. Holden, A. Golnik, C.T. Lin, and M. Cardona, *Phys. Rev. B* 61, 618 (2000).
- [53] G. Bums, F.H. Dacol, C. Feild, F. Holtzberg *Physica C* 181, 37 (1991).
- [54] D. van der Marel and A.A. Tsvetkov, *Czech. J. Phys.* 46, 3165, (1996).
- [55] D.M. unzar, C. Bernhard, A. Golnik, J. Humlíček, and M. Cardona, *Solid State Comm.* 112, 365 (1999).
- [56] C. Bernhard, D.M. unzar, A. Golnik, C.T. Lin, A. W. Ittlin, J. Humlíček, and M. Cardona *Phys. Rev. B* 62, 9138 (2000).
- [57] T. Timusk and C.C. Homes, *Solid State Communications*, (in press)
- [58] C. Bernhard, D.M. unzar, A. W. Ittlin, W. Koniig, A. Golnik, C.T. Lin, M. K. Kaser, Th. Wolf, G. Müller-Vogt, and M. Cardona *Phys. Rev. B* 59, R6631 (1999).
- [59] O.K. Andersen, O. Jepsen, A.J. Liechtenstein, and I.I. Mazin, *Phys. Rev. B* 49, 4145 (1994).
- [60] O.K. Andersen, *J. Phys. Chem. Solids* 56, 1573 (1995).
- [61] T. Xiang and J.M. Wheatley, *Phys. Rev. Lett.* 77, 4632 (1996).
- [62] A.V. Puchkov, P. Fournier, D.N. Basov, T. Timusk, A. Kapitulnik, N.N. Kolesnikov, *Phys. Rev. Lett.* 77, 3212, (1996).
- [63] J.W. Allen and J.C. Mikkelsen, *Phys. Rev. B* 15, 2952 (1977).
- [64] H. Mori, *Prog. Theor. Phys.* 34, 399 (1965).
- [65] W. Gotze and P. Wolfe, *Phys. Rev. B* 6, 1226 (1972).
- [66] S.V. Shulga, O.V. Dolgov, and E.G. Maksimov, *Physica C* 178, 266 (1991).
- [67] E.J. Singley, D.N. Basov, K. Kurahashi, T. Uefuji, and K. Yamada, *Phys. Rev. B* 64, 224503 (2001).
- [68] J.J. Tu, C.C. Homes, G.D. Gu, D.N. Basov, S.M. Loureiro, R.J. Cava, M. Strongin, *Phys. Rev. B* 66, 144514 (2002).
- [69] D.B. Tanner and T. Timusk, *Optical Properties of High-Temperature Superconductors*, in *Physical Properties of High Temperature Superconductors III* D.M. Ginsberg, editor, (World Scientific, Singapore, 1992) 105 pp.
- [70] F. Gao, D.B. Romero, D.B. Tanner, J. Talvacchio, and M.G. Forrester, *Phys. Rev. B* 47, 1036 (1993).
- [71] M.A. Quijada, D.B. Tanner, R.J. Kelley, M. O'Neill, H. Berger, and G. Maragari, *Phys. Rev. B* 60, 14917 (1999).
- [72] A.V. Puchkov, D.N. Basov, and T. Timusk, *J. Physics*,

- Condensed Matter, 8, 10049, (1996).
- [73] T. Startseva, R.A. Hughes, A.V. Puchkov, D.N. Basov, T. Timusk, and H.A. Mook, Phys. Rev. B 59, 7184, (1999).
  - [74] T. Startseva, T. Timusk, M. Okuya, T. Kimura, and K. Kishio, Physica C 321, 135, (1999).
  - [75] M. Dumm, D.N. Basov, S. Komiyama, Y. Abe, and Y. Ando, Phys. Rev. Lett. 88, 147003 (2002).
  - [76] J.J. McGuire, M. Windt, T. Startseva, T. Timusk, D. Colson, V. Viallet-Guillen, Phys. Rev. B 62, 8711 (2000).
  - [77] A. Sacuto, R. Combescot, N. Bonemps and C.A. Muller Phys. Rev. B 58 11721 (1998).
  - [78] M.-H. Julien, P. Carretta, M. Horvatic, C. Berthier, Y. Berthier, P. Segransan, A. Carrington, and D. Colson Phys. Rev. Lett. 76, 4238, (1996).
  - [79] A.J.M. Illis and H. Monien, Phys. Rev. Lett. 70, 2810 (1993).
  - [80] S. Ohsugi, Y. Kitaoka, K. Ishida, and K. Asayama, J. Phys. Soc. Japan, 60, 2351 (1991). comment weak pseudogap in HTSC La214
  - [81] B. Batlogg, H.Y. Hwang, H. Takagi, R.J. Cava, H.L. Kao, and J. Kwo, Physica C 235{240, 130 (1994).
  - [82] D.N. Basov, H.A. Mook, B. Dabrowski, and T. Timusk, Phys. Rev. B 52, R13141 (1995).
  - [83] S. Uchida, K. Tamasa, and S. Tajima, Phys. Rev. B 53, 14558 (1996).
  - [84] M. Reedyk and T. Timusk, Evidence for ab-plane Coupling to Longitudinal c-axis Phonons in High-T<sub>c</sub> Cuprate Superconductors, Phys. Rev. Lett. 69, 2705, 1992
  - [85] S. Tajima, (private communication)
  - [86] C.M. Vam, P.B. Littlewood, S. Schmitt-Rink, E. Abraham, and A.E. Ruckenstein, Phys. Rev. Lett. 63, 1996 (1989).
  - [87] M. Gurrvitch and A.T. Fiory, Phys. Rev. Lett. 59, 1337, 1987
  - [88] Z. Schlesinger, R.T. Collins, F. Holtzberg, C. Feild, S.H. Blanton, U. Welp, G.W. Crabtree, Y. Fang, and J.Z. Liu, Phys. Rev. Lett. 65, 801 (1990).
  - [89] It is clear that the gap in the scattering rate develops below 200 K and above the onset of superconductivity T<sub>c</sub> but there is an unfortunate lack of data between these two temperatures to determine the exact onset temperature of MFL scattering.
  - [90] E. Schachinger and J.P. Carbotte, Phys. Rev. B 64, 094501 (2001).
  - [91] For a review of the resonance peak in neutron scattering see P. Bourges, in The gap Symmetry and Fluctuations in High Temperature Superconductors, ed. J. Bok, G. Deutscher, D. Parrina, and S.A. Wolf, Plenum Press 1998, preprint cond-mat/9901333.
  - [92] D.A. Tanner, private communication.
  - [93] M. Eschrig and M.R. Norman, Phys. Rev. Lett. 85, 3261 (2000).
  - [94] A. Kaminski, J. Mesot, H. Fretwell, J.C. Camuzano, M.R. Norman, M. Randeria, H. Ding, T. Sato, T. Takahashi, T. Mochiku, K. Kadowaki, and H. Hoehst, Phys. Rev. Lett. 84, 1788 (2000).
  - [95] P.V. Bogdanov, A. Lanzara, S.A. Kellar, X.J. Zhou, E.D. Lu, W.J. Zheng, G. Gu, J.-I. Shimoyama, K. Kishio, H. Ikeda, R. Yoshizaki, Z. Hussain, and Z.X. Shen, Phys. Rev. Lett. 85, 2581 (2000).
  - [96] M.R. Norman, H. Ding, H. Fretwell, M. Randeria, J.C. Camuzano, Phys. Rev. B 60, 7585 (1999).
  - [97] A. Lanzara et al. Nature 412, 510 (2001).
  - [98] N.L. Wang, T. Timusk, J.P. Franck, P. Schweiss, M. Braden, A. Erb, The oxygen isotope effect in the ab-plane resistance of underdoped YBa<sub>2</sub>Cu<sub>3</sub>O<sub>7-x</sub>, Phys. Rev. Letters 89, 087003 (2002).
  - [99] H.F. Fong, P. Bourges, Y. Sidis, L.P. Regnault, J. Bossy, A. Ivanov, D.L. Mills, I.A. Aksay, and B. Keimer, Phys. Rev. Letters 82, 1939 (1999).
  - [100] G.-q. Zheng, T. Odaguchi, T. Mito, Y. Kitaoka, K. Asayama, and Y. Kodama, J. Phys. Soc. Japan 62, 2591 (1993).
  - [101] G.-q. Zheng, T. Odaguchi, Y. Kitaoka, K. Asayama, Y. Kodama, K. Mizuhashi, and S. Uchida, Physica C 263 367 (1996).
  - [102] For a review of the experimental NMR data on the pseudogap in high temperature superconductors see T. Timusk and B. Statt, Reports of Progress in Physics 62, 61 (1999).
  - [103] D.N. Basov and T. Timusk, B. Dabrowski and J.D. Jorgensen, Phys. Rev B 50, 3511 (1994).
  - [104] J.M. Harris, A.G. Loeser, D.S. Marshall, M.C. Schabel, and Z.-X. Shen Phys. Rev. B 54 R15665 (1996).
  - [105] A. Erb, E. Walker, and R. Flukiger, Physica C 258, 9 (1996), R.X. Liang, D.A. Bonn, and W.N. Hardy, Physica C 304, 105 (1998).